

Harmonics and intermodulation in subthreshold FitzHugh–Nagumo neuron

Wenjie Si, Jiang Wang, K. M. Tsang, and W. L. Chan

Citation: *Chaos* **19**, 033144 (2009); doi: 10.1063/1.3234239

View online: <http://dx.doi.org/10.1063/1.3234239>

View Table of Contents: <http://chaos.aip.org/resource/1/CHAOEH/v19/i3>

Published by the [American Institute of Physics](#).

Related Articles

Traffic-driven epidemic outbreak on complex networks: How long does it take?
Chaos **22**, 043146 (2012)

Epidemic variability in hierarchical geographical networks with human activity patterns
Chaos **22**, 023150 (2012)

Physics of cancer propagation: A game theory perspective
AIP Advances **2**, 011202 (2012)

Introduction to Focus Issue: Dynamics in Systems Biology
Chaos **20**, 045101 (2010)

Fibroblasts alter spiral wave stability
Chaos **20**, 045103 (2010)

Additional information on Chaos

Journal Homepage: <http://chaos.aip.org/>

Journal Information: http://chaos.aip.org/about/about_the_journal

Top downloads: http://chaos.aip.org/features/most_downloaded

Information for Authors: <http://chaos.aip.org/authors>

ADVERTISEMENT



AIP Advances

Submit Now

**Explore AIP's new
open-access journal**

- **Article-level metrics
now available**
- **Join the conversation!
Rate & comment on articles**

Harmonics and intermodulation in subthreshold FitzHugh–Nagumo neuron

Wenjie Si,¹ Jiang Wang,^{1,a)} K. M. Tsang,² and W. L. Chan²

¹*School of Electrical and Automation Engineering, Tianjin University, Tianjin 300072, China*

²*Department of Electrical Engineering, The Hong Kong Polytechnic University, Hong Kong*

(Received 26 March 2009; accepted 30 August 2009; published online 28 September 2009)

Intermodulation and harmonics are important in frequency analysis of nonlinear systems. In neuron research, most investigations are taken in studying synchronization between the external stimuli and the output of neuron, but harmonics and intermodulation are often ignored. In this paper, harmonics and intermodulation of the subthreshold FitzHugh–Nagumo neuron are investigated and their magnitudes are used to predict frequency response of the neuron. Furthermore, through analyzing the magnitudes of harmonics, the intrinsic frequencies of the neuron could be identified.

© 2009 American Institute of Physics. [DOI: [10.1063/1.3234239](https://doi.org/10.1063/1.3234239)]

A harmonic of a wave is a component frequency of the signal that is an integer multiple of the fundamental frequency, while intermodulation is the result of two or more signals of different frequencies being mixed together, forming additional signals at frequencies that are not, in general, at harmonic frequencies of either. Both harmonics and intermodulation are caused by nonlinear behaviors of systems. Recently, they are well investigated in biological applications such as improving human's hearing and vision system. However, in neuron models, harmonics and intermodulation are rarely concerned. Investigators always focus on the external synchronization between the input and output. In traditional study of the external synchronization, signals at continuous frequencies are introduced to stimulate neuron to get corresponding output. By calculating the spectrum or Fourier coefficient of the output at each input frequency, the frequency response is obtained. So harmonics and intermodulation of the applied input signal have been ignored. In this paper, a sinusoid input is applied to FitzHugh–Nagumo (FHN) neuron to make it remain in subthreshold oscillations and the corresponding harmonics and intermodulation are studied. They are incorporated to predict frequency response of the neuron. Also by identifying the maximum magnitude of harmonics, we can get the special input frequencies where the neuron could be more easily excited. Moreover, it demonstrates that the output response of a FHN neuron may not be maximum at the input frequency. Some output frequencies generated from harmonics or intermodulation may have significant effects on the output response which cannot be ignored in frequency analysis of the neuron.

I. INTRODUCTION

A harmonic of a wave is a component frequency of the signal that is an integer multiple of the fundamental frequency. For instance, given a signal with a fundamental angular frequency ω , its harmonics are given by ω , 2ω , 3ω , etc.

Being different from harmonics, intermodulation or intermodulation distortion happens when two or more signals at different frequencies are mixed together to stimulate a nonlinear system to form additional signals at frequencies that are not, in general, at the harmonic frequencies. Harmonics and intermodulation are caused by nonlinear behaviors of the signal processing being used. The theoretical outcome of these nonlinearities can be calculated by conducting a Volterra series of the characteristic, while the usual approximation of those nonlinearities is obtained by conducting a Taylor series.^{1,2} Existing methods to study nonlinear behavior of systems are based on transforming the Volterra kernels to the frequency domain to yield the generalized transfer functions. Although these approaches could characterize nonlinear system in the frequency domain properly, the available measurement techniques are all based on extending the classical linear fast Fourier transform algorithms to higher dimensions. Inevitably, it will increase the complexity and efforts in computing the nonlinear spectra. A methodology^{1,2} is introduced for analyzing unknown nonlinear systems in the frequency domain as an alternative to the nonparametric algorithms. The method is to fit a model to an unknown system and to apply probing method³ to obtain the nonlinear frequency responses.

Recently, the harmonics and intermodulation in vision and hearing systems have been well studied.^{4–9} As pointed out in some of these works, intermodulation distortion could possibly reduce the energy of pure tones at characteristic frequency in the vision or hearing systems. It also⁷ shows that significant spectral frequency-following responses are detected at harmonics close to formant peaks and at harmonics corresponding to cochlear intermodulation distortion products^{10,11} present that the cochlear microphonic potentials in homozygotes manifest harmonic and intermodulation distortion. It is impossible to list all articles on intermodulation and harmonics in nervous system. Although harmonics and intermodulation are well investigated in biological application, they are rarely discussed in frequency response analysis of neuron models. Investigators always focus on the synchronization between the output and the stimuli.^{12–19} In other words, they just pay attention to the output whose frequency

^{a)}Author to whom correspondence should be addressed. Electronic mail: jiangwang@tju.edu.cn.

matches the inputs and neglect harmonics and intermodulation of the input (fundamental) frequencies. In traditional synchronization study, the signals at continuous frequencies are introduced to stimulate the neuron. By calculating the output spectrum or Fourier coefficient at each input frequency, the frequency response of the neuron is obtained. So the harmonics and intermodulation of the applied signal have been ignored. In this paper, a sinusoid input is applied to FHN neuron to make it in subthreshold oscillation and the corresponding harmonics and intermodulation are calculated through the probing method to predict the frequency response of the neuron. By identifying the maximum magnitude responses of harmonics, we can get the characteristic frequencies where the neuron could get excited more easily.

This paper is organized as follows. Section II provides nonlinear frequency response functions while Sec. III, as the new contribution, shows the harmonics and intermodulation in the FHN neuron, which is excited by one or two sinusoid input stimuli. The last part is the conclusion.

II. NONLINEAR FREQUENCY RESPONSE FUNCTIONS

Based on the Volterra series, the traditional description of output of a nonlinear system with $u(t)$ as input is shown as follows:²⁰

$$y(t) = \sum_{n=1}^{\infty} \int_{-\infty}^{+\infty} \cdots \int h_n(\tau_1, \tau_2, \dots, \tau_n) \prod_{i=1}^n u(t - \tau_i) d\tau_i, \quad (1)$$

where $h_n(\tau_1, \tau_2, \dots, \tau_n)$ is the n th order Volterra kernel which can be visualized as a nonlinear impulse response function of order n . The n th order generalized frequency response function can be obtained by taking multiple Fourier transform of the n th order Volterra kernel,

$$H_n(\omega_1, \omega_2, \dots, \omega_n) = \int_{-\infty}^{+\infty} \cdots \int h_n(\tau_1, \dots, \tau_n) e^{-j(\omega_1 \tau_1 + \dots + \omega_n \tau_n)} d\tau_1 \cdots d\tau_n. \quad (2)$$

Equation (1) states that any time-invariant, nonlinear system can be modeled as an infinite sum of multidimensional convolution integrals of increasing order.

A. Computation of nonlinear frequency response functions

Probing or harmonic input method^{1,2} can be applied to obtain the steady-state output of a nonlinear system. If the input $u(t)$ is a sum of K exponentials given by

$$u(t) = \sum_{k=1}^K A_k e^{j\omega_k t}, \quad (3)$$

where A_k and ω_k represent the amplitude and angular frequency, respectively, the n th order output can be expressed²¹ as

$$y_n(t) = \sum_{k_1=1}^K \cdots \sum_{k_n=1}^K [A_{k_1} \cdots A_{k_n} H_n(\omega_{k_1}, \dots, \omega_{k_n})] e^{j(\omega_{k_1} + \dots + \omega_{k_n})t}, \quad (4)$$

where each permutation of $\omega_{k_1}, \dots, \omega_{k_n}$ in the argument of $H_n(\cdot)$ gives rise to a term in the n th order output and different terms may give rise to the same output angular frequency. If $y(t) = \sum_{n=1}^{\infty} y_n(t)$ contains no component with angular frequency $\omega_1 + \omega_2 + \dots + \omega_K$ other than those $K!$ terms in $y_n(t)$, the symmetrized n th order nonlinear transfer function $H_n(\omega_1, \dots, \omega_n)$ can be obtained by the probing input method by equating coefficients of $K! e^{j(\omega_1 + \dots + \omega_K)t}$ in the system output when the input is defined as in Eq. (3) with $A_{k_i} = 1$.^{11,22} It has been shown in Ref. 21 that if the angular frequencies $\{\omega_1, \omega_2, \dots, \omega_k\}$ form an angular frequency base, the sum of all terms with angular frequency ω_M in Eq. (4) for the n th output component $y_n(t)$ denoted by $y_n(t; \omega_M)$ is given as follows:

$$y_n(t; \omega_M) = n! \left[\prod_{k=1}^K \frac{A_k^{m_k}}{m_k} \right] H_n(m_1\{\omega_1\}, \dots, m_k\{\omega_k\}) e^{j\omega_M t}, \quad (5)$$

where $m_k\{\omega_k\}$ denotes m_k consecutive arguments in $H_n(\cdot)$ with the same angular frequency ω_k and $\sum_{k=1}^K m_k = n$. Since $y_n(t)$ consists of all possible angular frequency mixes that satisfy $\sum_{k=1}^K m_k = n$, Eq. (4) can be expressed as

$$y_n(t) = \sum_{\text{all possible } M} y_n(t; \omega_M) = \sum_{m_1=0}^n \cdots \sum_{m_k=0}^n y_n(t; \omega_M), \quad (6)$$

where the terms do not have overlapping angular frequency components.

In actual practice, the input equation (3) cannot be realized and a more realistic input composed of K different sinusoids²¹ is presented as follows:

$$u(t) = \sum_{i=1}^K |A_i| \cos(\omega_i t + \angle A_i) = \sum_{i=1}^K \left[\frac{A_i}{2} e^{j\omega_i t} + \frac{A_i^*}{2} e^{-j\omega_i t} \right], \quad (7)$$

where $|A_i|$, $\angle A_i$, and A_i^* are the amplitude, phase, and complex conjugate of A_i , respectively. By definition $A_{-i} = A_i^*$ and $\omega_{-i} = -\omega_i$, Eq. (7) can be expressed as

$$u(t) = \sum_{\substack{i=-K \\ i \neq 0}}^K \frac{A_i}{2} e^{j\omega_i t}. \quad (8)$$

Then Eq. (5) could be rewritten as follows:

$$y_n(t; \omega_M) = \frac{n!}{2^n} \left[\prod_{\substack{i=-K \\ i \neq 0}}^K \frac{A_i^{m_i}}{m_i} \right] H_n(m_{-K}\{\omega_{-K}\}, \dots, m_{-1}\{\omega_{-1}\}, \dots, m_k\{\omega_k\}) \times e^{j\omega_M t}. \quad (9)$$

Equation (9) illustrates that the output components ($y_n(t)$ s) are generated by the n th order frequency response functions of the system. When a sum of K sinusoids is applied to a nonlinear system, $y_n(t)$ consists of all possible

combinations of the input angular frequencies $\{-\omega_K, \dots, -\omega_1, \omega_1, \dots, \omega_K\}$ with the number of n . Because $\{\omega_{-K}, \dots, \omega_{-1}, \omega_1, \dots, \omega_K\}$ is not an angular frequency base, different module vectors of the same order can produce the same output angular frequency. Equation (9) can be used to predict how harmonics and intermodulation arise in the response of nonlinear systems.

B. Harmonics

Harmonics are frequency components which are equal to multiples of the fundamental input frequencies. The l th harmonics are the frequency component oscillating at l times the input frequency. Assume that the input is a single sinusoid, namely, $u(t) = |A| \cos(\omega t + \angle A)$, and consider just the n th order output response $y_n(t)$. Because the input is a single sinusoid, the two input angular frequencies are $-\omega$ and ω .

From Eq. (9), the n th order output component that corresponds to an angular frequency mix $\omega_M = (m_1 - m_{-1})\omega$ is given as follows:

$$y_n(t; \omega_M) = \frac{n!}{2^n m_{-1}! m_1!} (A^*)^{m_{-1}} (A)^{m_1} H_n(m_{-1}\{-\omega\}m_1\{\omega\}) \times e^{j(m_1 - m_{-1})\omega t}. \tag{10}$$

The exponential term $e^{j(m_1 - m_{-1})\omega t}$ in Eq. (10) clearly reveals that the output consists of either the fundamental constant component or harmonics of the input angular frequency depending upon the value of the positive integers m_1 and m_{-1} . The l th order harmonic is yielded when $m_1 - m_{-1} = l$. Because the output of a real system is real for real inputs and the complex terms in $y_n(t)$ appear in conjugate pairs, the sinusoidal response at angular frequency ω_M can thus be obtained by combining Eq. (10) with its complex conjugate,

$$\begin{aligned} \tilde{y}_n(t; \omega_M) &= y_n(t; \omega_M) + y_n^*(t; \omega_M) \\ &= y_n(t; \omega_M) + y_n(t; -\omega_M) \\ &= 2 \operatorname{Re}\{y_n(t; \omega_M)\} \\ &= \operatorname{Re}\left\{ \frac{n!}{2^{n-1} m_{-1}! m_1!} (A^*)^{m_{-1}} (A)^{m_1} \right. \\ &\quad \left. \times H_n(m_{-1}\{-\omega\}, m_1\{\omega\}) e^{j(m_1 - m_{-1})\omega t} \right\}, \end{aligned} \tag{11}$$

where $\tilde{y}_n(t; \omega_M)$ denotes the n th order sinusoidal response at angular frequency ω_M . From Eq. (11) the magnitude of the l th harmonic is

$$\begin{aligned} |E_l| &= |A|^{(l)} \left| \frac{1}{2^{(l-1)}} H_l(l\{\omega\}) \right. \\ &\quad \left. + \frac{l+2}{2^{(l+1)}} |A|^2 H_{l+2}(-\omega, (l+1)\{\omega\}) + \dots \right|. \end{aligned} \tag{12}$$

C. Intermodulation

The process of two or more signals combined in a nonlinear manner to produce new frequency components is termed intermodulation. If a nonlinear system is excited by a sum of K sinusoidal inputs as expressed in Eq. (8), the an-

gular frequency mix represented by the n th order module vector $M = (m_{-K}, \dots, m_{-1}, m_1, \dots, m_K)$ generates a nonlinear angular frequency component at the intermodulation angular frequency as $\omega_M = (m_1 - m_{-1})\omega_1 + \dots + (m_K - m_{-K})\omega_K$. Noteworthy, the positive integers in the vector M sum to n . Because the output of a real system is real for real inputs, the n th order real output response at ω_M is given by

$$\begin{aligned} \tilde{y}_n(t; \omega_M) &= 2 \operatorname{Re}\{y_n(t; \omega_M)\} \\ &= \operatorname{Re}\left\{ \frac{n!}{2^{n-1}} \left(\prod_{\substack{i=-K \\ i \neq 0}}^K \frac{A_i^{m_i}}{m_i!} \right) \right. \\ &\quad \left. \times H_n(m_{-K}\{\omega_{-K}\}, \dots, m_{-1}\{\omega_{-1}\}, m_1\{\omega_1\}, \dots, m_K\{\omega_K\}) \right. \\ &\quad \left. \times e^{j\omega_M t} \right\}. \end{aligned} \tag{13}$$

The effect of each intermodulation term can be examined by inspecting the magnitude associated with the intermodulation term at angular frequency ω_j , which is presented as follows:

$$\operatorname{Mag}(\omega_j) = \left| \sum_{n=1}^{\infty} \sum_{\substack{\text{All possible } M \\ \text{such that } \omega_M = \omega_j}} \tilde{y}_n(t; \omega_M) \right|. \tag{14}$$

III. NONLINEAR FREQUENCY RESPONSE FUNCTIONS FOR FHN NEURON

The FHN neuron is modeled as

$$\begin{aligned} \varepsilon \dot{x}(t) &= -y(t) - \frac{1}{3}x^3(t) + x(t), \\ \dot{y}(t) &= x(t) + a + u(t), \end{aligned} \tag{15}$$

where the neuron membrane voltage $x(t)$ and the recovery variable $y(t)$ are considered as dimensionless variables. ε and a are the time scale and bifurcation parameter, respectively. For a FHN neuron without any external input, if $|a| > 1$ the system has only one stable fixed point corresponding to the quiescent state of the system, while if $|a| < 1$ there exists a globally stable limit cycle. $u(t)$ is the external input. We differentiate Eq. (15) with respect to time and get $\varepsilon \dot{x}(t) = -x(t) - a - u(t) - x^2(t)\dot{x}(t) + \dot{x}(t)$ which could be converted to

$$\varepsilon \dot{z}(t) + (z^2(t) - 2az(t) + a^2 - 1)\dot{z}(t) + z(t) = -u(t) \tag{16}$$

by introducing a new variable $z(t) = x(t) + a$.

As the difference between the variables $x(t)$ and $z(t)$ is the constant offset a , the probing method can then be applied to Eq. (16) to obtain the nonlinear frequency response functions. The procedure is begun by setting $K = 1, A_k = 1, \omega_k = \omega$ in Eq. (8) to define the first probing input $u(t) = e^{j\omega t}$. According to Eq. (11) with $n = 1$,

$$z(t) = H_1(\omega) e^{j\omega t}, \tag{17}$$

and hence

$$\dot{z}(t) = (j\omega)H_1(\omega)e^{j\omega t}, \quad \ddot{z}(t) = (j\omega)^2H_1(\omega)e^{j\omega t}. \quad (18)$$

Substituting Eqs. (17) and (18) into Eq. (16) gives

$$\varepsilon(j\omega)^2H_1(\omega)e^{j\omega t} + (a^2 - 1)(j\omega)H_1(\omega)e^{j\omega t} + H_1(\omega)e^{j\omega t} = -e^{j\omega t}, \quad (19)$$

and equating coefficients of $e^{j\omega t}$ on both sides yields

$$H_1(\omega) = -\frac{1}{\varepsilon(j\omega)^2 + j(a^2 - 1)\omega + 1}. \quad (20)$$

Then probe with two inputs by setting $K=2, A_k=1 \forall k$ in Eq. (3),

$$u(t) = e^{j\omega_1 t} + e^{j\omega_2 t}. \quad (21)$$

According to Eq. (4) with $n=2$, we could get

$$\begin{aligned} y(t) &= \sum_{n=1}^2 y_n(t) \\ &= H_1(\omega_1)e^{j\omega_1 t} + H_1(\omega_2)e^{j\omega_2 t} + 2! H_1(\omega_1, \omega_2)e^{j(\omega_1+\omega_2)t} \\ &\quad + H_2(\omega_1, \omega_1)e^{j(2\omega_1)t} + H_2(\omega_2, \omega_2)e^{j(2\omega_2)t}. \end{aligned} \quad (22)$$

Differentiating Eq. (22) with respect to time obtains its first and second order derivatives, and substituting them into Eq. (16) followed by equating coefficients of $2!e^{j(\omega_1+\omega_2)t}$ yields

$$H_2(\omega_1, \omega_2) = -aj(\omega_1 + \omega_2)H_1(\omega_1)H_1(\omega_2)H_1(\omega_1 + \omega_2). \quad (23)$$

Continuing the procedures by probing with three, four, and five exponentials and equating coefficients of $3!e^{j(\omega_1+\omega_2+\omega_3)t}$, $4!e^{j(\omega_1+\omega_2+\omega_3+\omega_4)t}$, and $5!e^{j(\omega_1+\omega_2+\omega_3+\omega_4+\omega_5)t}$, respectively, on both sides of Eq. (16) yields the third, fourth, and fifth frequency response functions, see Eqs. (A1)–(A3) in the Appendix.

Notice that the procedure can be continued indefinitely to calculate higher order nonlinear frequency response functions, which will be composed by the lower order functions. Although the Volterra expansion is infinite because of the nonlinearity in the model and each kernel of the expansion could contribute to the output, the influence of high order kernels will be vanishing with the amplitude of excitation being less than 1.

A. Case study 1

The input $u(t)$ is chosen as a single cosine signal, namely, $A \cos(\omega t)$, where A and ω are the amplitude and the angular frequency, respectively. So the two input angular frequency components are $-\omega$ and ω . The n th order module vector of the input angular frequencies is therefore of the form $M=(m_{-1}, m_1)$, where $m_{-1}+m_1=n$. The parameters of the FHN neuron are chosen as $\varepsilon=0.01$ and $a=1.01$. Table I shows the first to the fifth harmonic magnitudes of the output. It has been assumed that the input amplitude A is so small that the influence of the frequency response functions, which is higher than the fifth order, could be neglected. To evaluate the effect of input amplitude and magnitude of harmonics on output response of FHN neuron, the effective gain of harmonics is defined as follows:

TABLE I. Magnitude responses of harmonics.

Magnitude response of harmonics	
$ E_1(\omega) $	$ AH_1(\omega) + \frac{3}{4}A^3H_3(-\omega, \omega, \omega) + \frac{5}{8}A^5H_5(-\omega, -\omega, \omega, \omega, \omega) $
$ E_2(\omega) $	$ \frac{1}{2}A^2H_2(\omega, \omega) + \frac{1}{2}A^4H_4(-\omega, \omega, \omega, \omega) $
$ E_3(\omega) $	$ \frac{1}{4}A^3H_3(\omega, \omega, \omega) + \frac{5}{16}A^5H_5(-\omega, \omega, \omega, \omega, \omega) $
$ E_4(\omega) $	$ \frac{1}{8}A^4H_4(\omega, \omega, \omega, \omega) $
$ E_5(\omega) $	$ \frac{1}{16}A^5H_5(\omega, \omega, \omega, \omega, \omega) $

$$|G_l(\omega)| = \frac{|E_l(\omega)|}{A}, \quad (24)$$

where $E_l(\omega)$ denotes the magnitude of harmonics and A is the input amplitude.

Figure 1 shows the effective gain spectra of harmonics for different input amplitudes. When the input amplitude is close to zero, the output is dominated by the first harmonic because the effective gains of higher order harmonics are close to zero. From the effective gain spectrum of the first harmonic in Fig. 1(a), a spectral peak is identified at about 9.8 rad/s, which has been reported as the Carnard oscillation angular frequency in Ref. 23. From Figs. 1(b)–1(e), as the input amplitude increases up to 0.01, the second, third, fourth, and fifth order harmonics start to have effect on the output response of the neuron. Spectral peaks at 5.0 and 9.8 rad/s are identified from the effective gain of the second harmonic. 3.4, 4.9, and 9.8 rad/s are identified for the third harmonic; 3.3, 5.1, and 9.8 rad/s are identified for the fourth harmonic; and 2.5, 5, and 9.8 rad/s are identified for the fifth harmonic. On top of the Carnard oscillation angular frequency around 9.8 rad/s, the FHN neuron can easily get excited at other angular frequencies such as 2.5, 3.4, and 5 rad/s based on the identified spectral peaks from the gain spectra of higher harmonics.

To verify if the effective gain spectra of higher harmonics could predict the output response of FHN neuron, a sinusoid with amplitude of 0.01 and angular frequency of 5 rad/s was used as the input stimuli. Figure 2 shows the output response of the FHN neuron, and clearly, higher order frequency response functions have very little effects on the output response. Figure 3 is obtained in the same stimulus as Fig. 2. Figure 3(a) shows the spectrum of the output signal based on Table I and Fig. 3(b) shows the spectrum of the output signal based on the Fourier analysis.

To evaluate the response of the output frequency to the input frequency based on Fourier analysis, the Fourier coefficient Q of the output is calculated at the input angular frequency ω as follows:²³

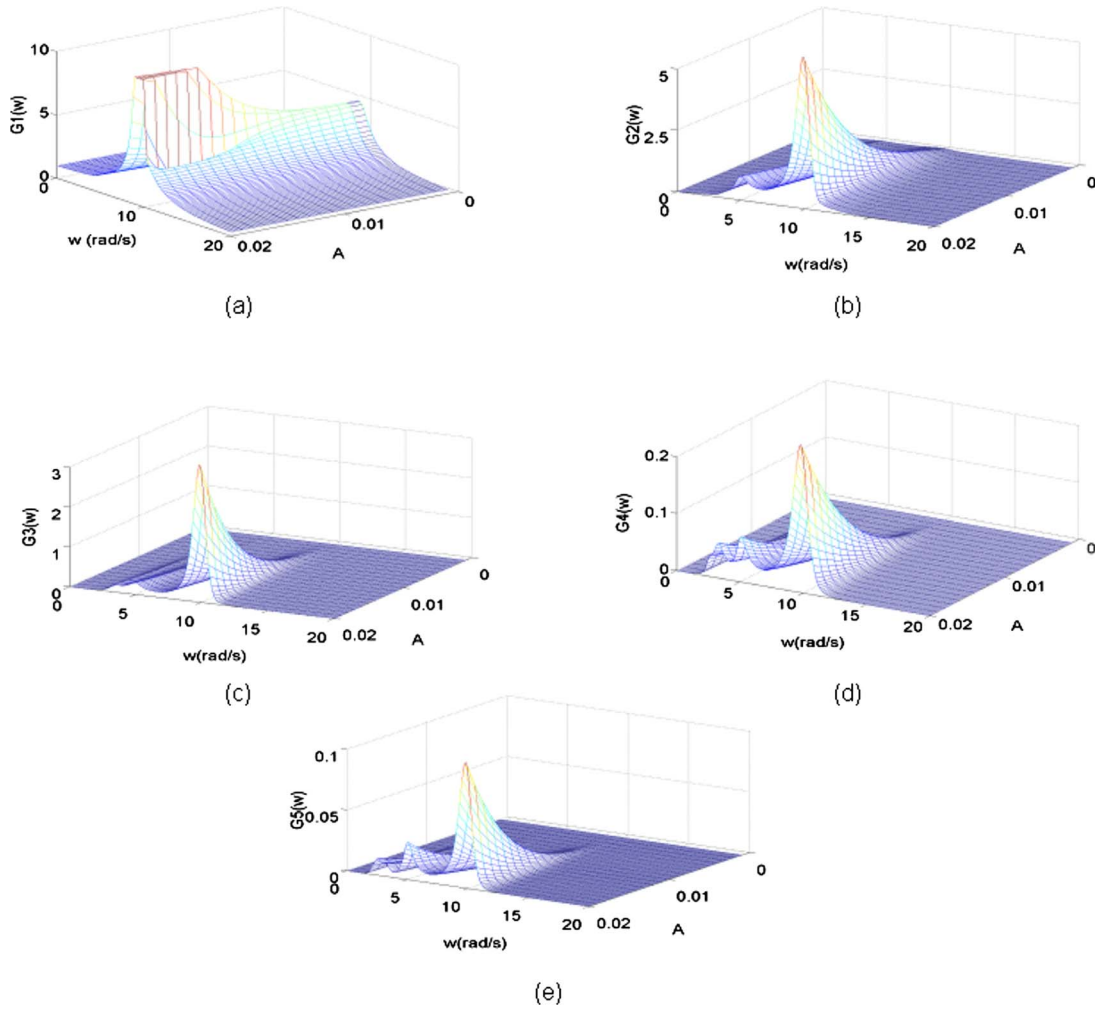


FIG. 1. (Color online) The effective gain spectra for higher harmonics at different amplitudes of input: (a) first harmonic, (b) second harmonic, (c) third harmonic, (d) fourth harmonic, and (e) fifth harmonic.

$$\begin{aligned}
 Q_{\sin} &= \frac{\omega}{2\pi n} \int_0^{2\pi n/\omega} 2x(t)\sin(\omega t)dt, \\
 Q_{\cos} &= \frac{\omega}{2\pi n} \int_0^{2\pi n/\omega} 2x(t)\cos(\omega t)dt, \\
 Q &= \sqrt{Q_{\sin}^2 + Q_{\cos}^2},
 \end{aligned} \tag{25}$$

where n is the number of periods $2\pi/\omega$ covered by the integration time. The Q parameter is a much more compact tool

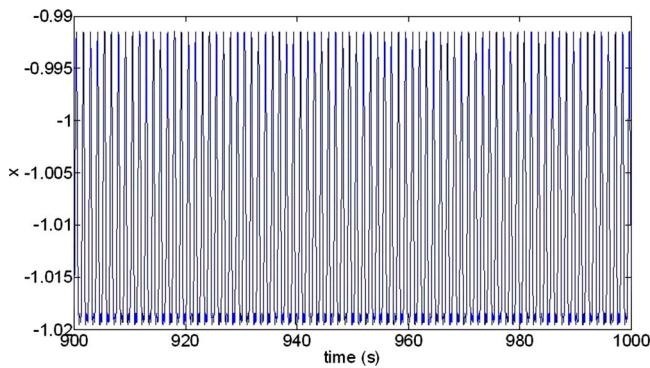


FIG. 2. (Color online) Output response (namely, spike train) of FHN neuron with $A=0.01$ and $\omega=5$ rad/s.

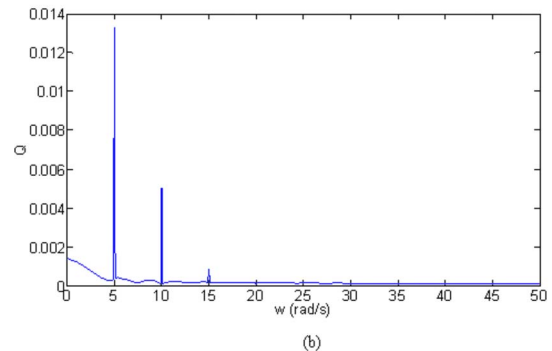
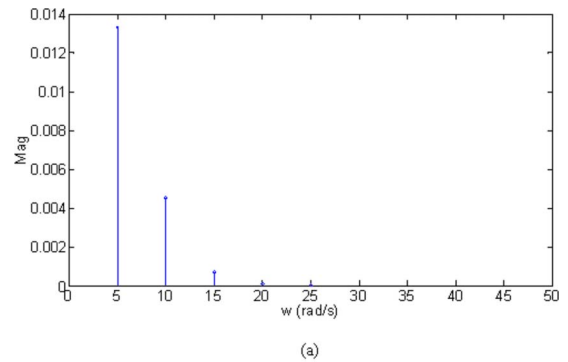


FIG. 3. (Color online) Output spectra. (a) Theoretical output spectra calculated by Eq. (12). (b) Fourier output spectra derived by simulations.

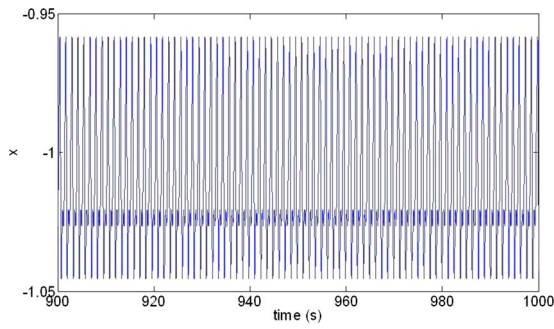


FIG. 4. (Color online) Output response of FHN neuron with $A=0.02$ and $\omega=5$ rad/s.

than the power spectrum.^{24,25} The authors carried out a lot of simulations by differing input angular frequency continuously (e.g., 0.1–50 rad/s) to obtain the output, and by calculating the Fourier coefficient Q of each output at the corresponding input angular frequency, the Fourier spectra could be gotten. Obviously, according to Fig. 3, theoretical values based on Table I agree with the values obtained from Fourier analysis. Then the input amplitude is increased to 0.02 and the output response of the FHN neuron is shown in Fig. 4. At this situation, the higher order harmonics begin to have effects on the output response. Figure 5 shows the spectra of the output signal based on Table I and Fourier analysis. The second and third harmonics are found to have significant effects on the output response because their magnitudes are comparable to the fundamental input angular frequency at 5 rad/s. Noteworthy, if the neuron is not excited at either one of the angular frequencies where identified spectral peaks

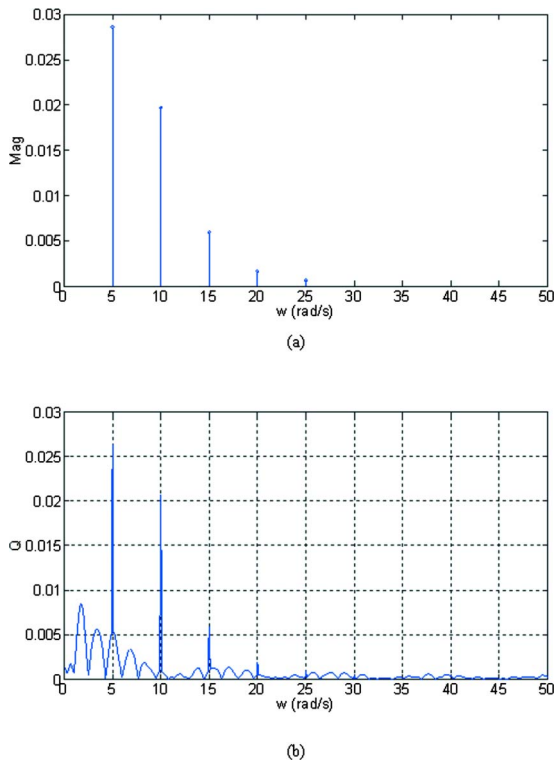


FIG. 5. (Color online) Output spectra. (a) Theoretical output spectra calculated by Eq. (12). (b) Fourier output spectra derived by simulations.

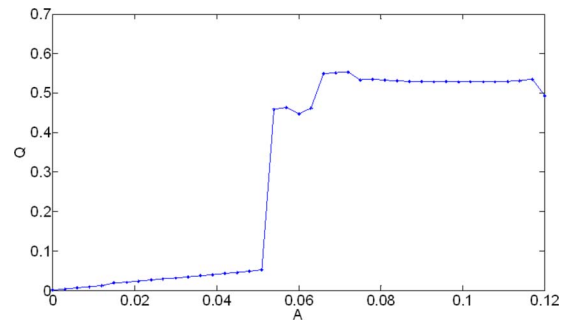


FIG. 6. (Color online) The spectra of the output signal based on the Fourier analysis with angular frequency of the input being 1 rad/s.

occur, synchronization between the input and output will be in a low level. Figure 6 shows the spectrum of the output signal based on Fourier analysis when the input angular frequency is 1 rad/s. Figure 7 shows the output spectra when the input angular frequency is one of the identified angular frequencies, for instance, 5 rad/s. According to the two plots, synchronization between the input and output could happen more easily when the input angular frequency arrives at 5 rad/s.

B. Case study 2

The parameters of the FHN neuron are chosen as $\epsilon=0.1$ and $a=1.01$. In Ref. 23, the authors carried out a lot of simulations for different input stimuli whose angular frequencies are from 0.1 to 5 rad/s and reported that the resonant angular frequencies of the neuron are 1.4 rad/s and another value, which is between 2.6 and 2.9 rad/s approximately. To demonstrate whether the two resonant angular frequencies can be captured by the frequency response functions, the effective gains of higher harmonics are calculated. Figure 8 shows the effective gain spectra for higher harmonics with different input amplitudes. From the effective gain spectrum of the first order harmonic, the resonant peak around 3.2 rad/s can be identified. Besides 3.2 rad/s, spectral peaks at 1.6 rad/s and lower angular frequencies also appear in the effective gain spectra of second and higher harmonics. Moreover, it can be seen that the effective magnitudes of harmonics at the identified angular frequencies,

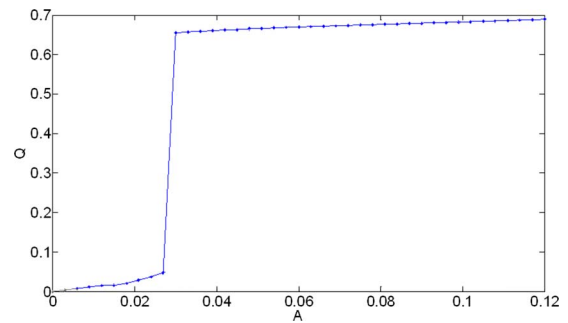


FIG. 7. (Color online) The spectra of the output when the input angular frequency is one of the identified values, i.e., 5 rad/s.

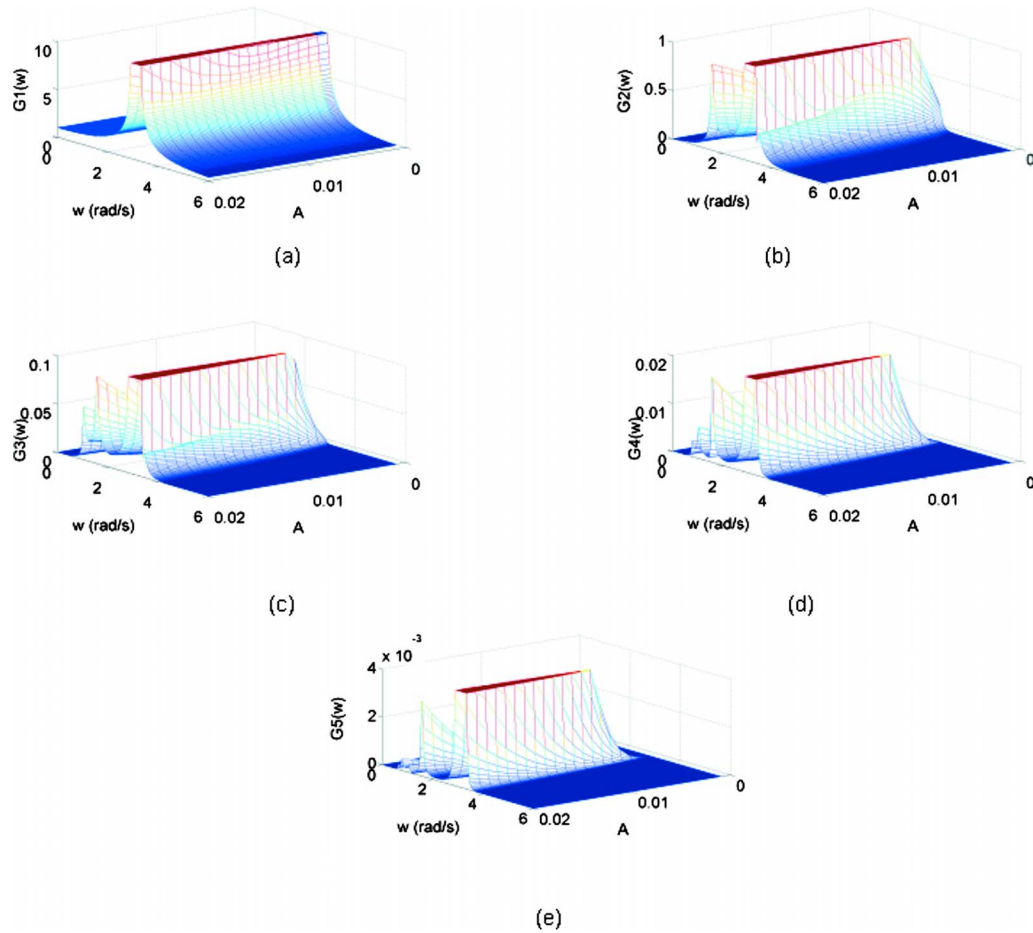


FIG. 8. (Color online) The effective gain spectra for higher harmonics at different amplitudes of input: (a) first harmonic, (b) second harmonic, (c) third harmonic, (d) fourth harmonic, and (e) fifth harmonic.

which are lower than 1.6 rad/s, are very small. So the two resonant frequencies reported in Ref. 23 can be easily identified by the frequency response functions. The advantage of using the frequency response functions in interpreting output response of FHN neurons is that the special frequency of the input stimuli, which could excite the neuron more easily, can be identified without performing any simulations.

C. Case study 3

To study the intermodulation effects of FHN neuron, the input stimuli composed of two sinusoids are chosen. The input is set to be $u(t) = A \cos(\omega_1 t) + A \cos(\omega_2 t)$ with $A = 0.02$. The two input angular frequencies are set as $\omega_1 = 2$ rad/s and $\omega_2 = 3$ rad/s, promising they are not integer multiple of each other. Table II shows the magnitude responses of all possible output frequencies.

The parameters of the FHN neuron are chosen as $\varepsilon = 0.01$ and $a = 1.01$. Figure 9 shows the output response of the neuron and Fig. 10 shows the output spectrum based on Table II and Fourier analysis. A comparison of the two results reveals that the nonlinear frequency response functions can capture the output response of FHN neuron very well.

A repeat of the analysis on another FHN neuron with $\varepsilon = 0.1$ and $a = 1.01$ shown in Figs. 11 and 12 demonstrates similar results.

IV. CONCLUSION

The probing method has been successfully applied to a subthreshold FHN neuron to extract their nonlinear frequency response functions. The effectiveness of the extracted nonlinear frequency response functions in predicting output responses of FHN neurons has been verified by carrying Fourier analysis on the output responses. Furthermore, the frequencies where the neuron can easily get excited could be identified from the effective gain spectra of harmonics, as well as the effect of input amplitude on output response of the FHN neuron.

When applying a sinusoid input to a FHN neuron and making it in the subthreshold oscillation, it demonstrates that the output response of the neuron may not be maximum at the frequency, which is similar to the input. Sometimes other output frequencies generated from harmonics or intermodulation may have apparent effects on the output response and these effects cannot be ignored in the analysis of FHN neurons.

ACKNOWLEDGMENTS

This work is supported by the Key NSFC of China (Grant No. 50537030), NSFC (Grant Nos. 50707020, 50907044, and 60901035), and NSF for Postdoctoral Scientists of China (Grant Nos. 20070410756, 200801212,

TABLE II. Magnitude responses of all output frequencies.

Output frequency (rad/s)	Magnitude of output response
1	$ A^2H_2(-\omega_1, \omega_2) + \frac{3}{4}A^3H_3(\omega_1, \omega_1, -\omega_2) + \frac{3}{2}A^4H_4(-\omega_1, -\omega_2, \omega_2, \omega_2) + \frac{3}{2}A^4H_4(-\omega_1, -\omega_1, \omega_1, \omega_2) + \frac{5}{4}A^5H_5(-\omega_1, \omega_1, \omega_1, \omega_1, -\omega_2) + \frac{15}{8}H_5(\omega_1, \omega_1, -\omega_2, -\omega_2, \omega_2) $
2	$ AH_1(\omega_1) + \frac{3}{2}A^3H_3(\omega_1, -\omega_2, \omega_2) + \frac{3}{4}A^3H_3(-\omega_1, \omega_1, \omega_1) + \frac{3}{4}A^4H_4(-\omega_1, -\omega_1, \omega_2, \omega_2) + \frac{15}{4}A^5H_5(-\omega_1, \omega_1, \omega_1, -\omega_2, \omega_2) + \frac{5}{8}A^5H_5(-\omega_1, -\omega_1, \omega_1, \omega_1, \omega_1) + \frac{15}{8}A^5H_5(\omega_1, -\omega_2, -\omega_2, \omega_2, \omega_2) $
3	$ AH_1(\omega_2) + \frac{3}{2}A^3H_3(-\omega_2, \omega_2, \omega_2) + \frac{3}{4}A^3H_3(-\omega_1, \omega_1, \omega_2) + \frac{3}{4}A^4H_4(\omega_1, \omega_1, \omega_1, -\omega_2) + \frac{15}{4}A^5H_5(-\omega_1, \omega_1, -\omega_2, \omega_2, \omega_2) + \frac{5}{8}A^5H_5(-\omega_1, -\omega_1, \omega_1, \omega_1, \omega_2) + \frac{15}{8}A^5H_5(-\omega_2, -\omega_2, \omega_2, \omega_2, \omega_2) $
4	$ \frac{1}{2}A^2H_2(\omega_1, \omega_1) + \frac{3}{4}A^3H_3(-\omega_1, \omega_2, \omega_2) + \frac{1}{2}A^4H_4(-\omega_1, \omega_1, \omega_1, \omega_1) + \frac{3}{2}A^4H_4(\omega_1, \omega_1, -\omega_2, \omega_2) + \frac{5}{4}A^5H_5(-\omega_1, -\omega_2, \omega_2, \omega_2, \omega_2) + \frac{15}{8}A^5H_5(-\omega_1, -\omega_1, \omega_1, \omega_2, \omega_2) $
5	$ A^2H_2(\omega_1, \omega_2) + \frac{3}{2}A^4H_4(-\omega_1, \omega_1, \omega_1, \omega_2) + \frac{3}{2}A^4H_4(\omega_1, -\omega_2, \omega_2, \omega_2) + \frac{5}{16}A^5H_5(\omega_1, \omega_1, \omega_1, \omega_1, -\omega_2) + \frac{5}{8}A^5H_5(-\omega_1, -\omega_1, \omega_2, \omega_2, \omega_2) $
6	$ \frac{1}{2}A^2H_2(\omega_2, \omega_2) + \frac{1}{4}A^3H_3(\omega_1, \omega_1, \omega_1) + \frac{1}{2}A^4H_4(-\omega_2, \omega_2, \omega_2, \omega_2) + \frac{3}{2}A^4H_4(-\omega_1, \omega_1, \omega_2, \omega_2) + \frac{5}{16}A^5H_5(-\omega_1, \omega_1, \omega_1, \omega_1, \omega_1) + \frac{5}{4}A^5H_5(\omega_1, \omega_1, \omega_1, -\omega_2, \omega_2) $
7	$ \frac{3}{4}A^3H_3(\omega_1, \omega_1, \omega_2) + \frac{1}{2}A^4H_4(-\omega_1, \omega_2, \omega_2, \omega_2) + \frac{5}{4}A^5H_5(-\omega_1, \omega_1, \omega_1, \omega_1, \omega_2) + \frac{15}{8}A^5H_5(\omega_1, \omega_1, -\omega_2, \omega_2, \omega_2) $
8	$ \frac{3}{4}A^3H_3(\omega_1, \omega_2, \omega_2) + \frac{1}{8}A^4H_4(\omega_1, \omega_1, \omega_1, \omega_1) + \frac{15}{8}A^5H_5(-\omega_1, \omega_1, \omega_1, \omega_2, \omega_2) + \frac{5}{4}H_5(\omega_1, -\omega_2, \omega_2, \omega_2, \omega_2) $
9	$ \frac{1}{4}A^3H_3(\omega_2, \omega_2, \omega_2) + \frac{1}{2}A^4H_4(\omega_1, \omega_1, \omega_1, \omega_2) + \frac{5}{4}A^5H_5(-\omega_1, \omega_1, \omega_2, \omega_2, \omega_2) + \frac{5}{16}H_5(-\omega_2, \omega_2, \omega_2, \omega_2, \omega_2) $
10	$ \frac{3}{4}A^4H_4(\omega_1, \omega_1, \omega_2, \omega_2) + \frac{5}{16}A^5H_5(-\omega_1, \omega_2, \omega_2, \omega_2, \omega_2) + \frac{1}{16}A^5H_5(\omega_1, \omega_1, \omega_1, \omega_1, \omega_1) $
11	$ \frac{1}{2}A^4H_4(\omega_1, \omega_2, \omega_2, \omega_2) + \frac{5}{16}H_5(\omega_1, \omega_1, \omega_1, \omega_1, \omega_2) $
12	$ \frac{1}{8}H_4(\omega_2, \omega_2, \omega_2, \omega_2) + \frac{5}{8}H_5(\omega_1, \omega_1, \omega_1, \omega_2, \omega_2) $
13	$ \frac{5}{8}H_5(\omega_1, \omega_1, \omega_2, \omega_2, \omega_2) $
14	$ \frac{5}{16}H_5(\omega_1, \omega_2, \omega_2, \omega_2, \omega_2) $
15	$ \frac{1}{16}H_5(\omega_2, \omega_2, \omega_2, \omega_2, \omega_2) $

20080430731, and 20080430090). K.M.T. and W.L.C. gratefully acknowledge the support of the Hong Kong Polytechnic University.

APPENDIX: THE HIGHER ORDER FREQUENCY RESPONSE FUNCTION

1. Third order frequency response function

$$\alpha_3 = H_1(\omega_1)H_1(\omega_2)H_1(\omega_3) - 2a(H_1(\omega_1)H_2(\omega_2, \omega_3) + H_1(\omega_2)H_2(\omega_1, \omega_3) + H_1(\omega_3)H_2(\omega_1, \omega_2)), \tag{A1}$$

$$H_3(\omega_1, \omega_2, \omega_3) = -2j(\omega_1 + \omega_2 + \omega_3)\alpha_3 / (6\epsilon(j(\omega_1 + \omega_2 + \omega_3))^2 + 6(a^2 - 1)(j(\omega_1 + \omega_2 + \omega_3)) + 6).$$

2. Fourth order frequency response function

$$\alpha_4 = -2a(4j(\omega_1 + \omega_2 + \omega_3 + \omega_4)(H_2(\omega_1, \omega_2)H_2(\omega_3, \omega_4) + H_2(\omega_1, \omega_3)H_2(\omega_2, \omega_4) + H_2(\omega_1, \omega_4)H_2(\omega_2, \omega_3))) - 12aj(\omega_1 + \omega_2 + \omega_3 + \omega_4)(H_1(\omega_1)H_3(\omega_2, \omega_3, \omega_4) + H_1(\omega_2)H_3(\omega_1, \omega_3, \omega_4) + H_1(\omega_3)H_3(\omega_1, \omega_2, \omega_4) + H_1(\omega_4)H_3(\omega_1, \omega_2, \omega_3)),$$

$$\beta_4 = 4j((\omega_3 + \omega_4)H_1(\omega_1)H_1(\omega_2)H_2(\omega_3, \omega_4) + (\omega_2 + \omega_4) \times H_1(\omega_1)H_1(\omega_3)H_2(\omega_2, \omega_4) + (\omega_2 + \omega_3)H_1(\omega_1)H_1(\omega_4) \times H_2(\omega_2, \omega_3) + (\omega_1 + \omega_4)H_1(\omega_2)H_1(\omega_3)H_2(\omega_1, \omega_4) + (\omega_1 + \omega_3)H_1(\omega_2)H_1(\omega_4)H_2(\omega_1, \omega_3) + (\omega_1 + \omega_2)H_1(\omega_3)H_1(\omega_4)H_2(\omega_1, \omega_2)),$$

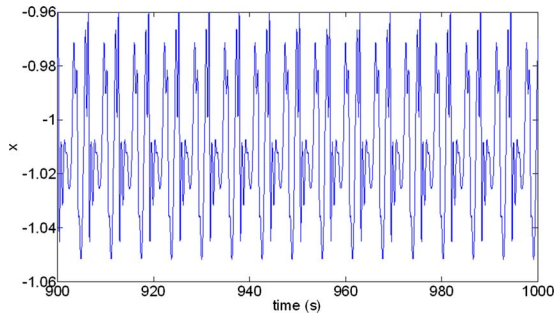
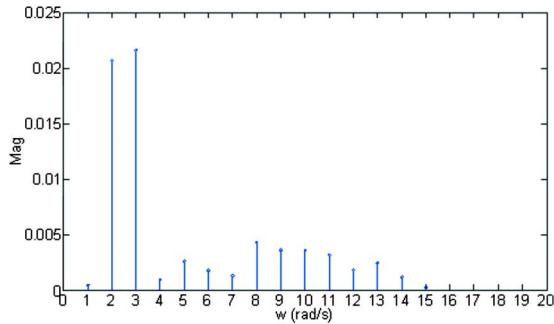
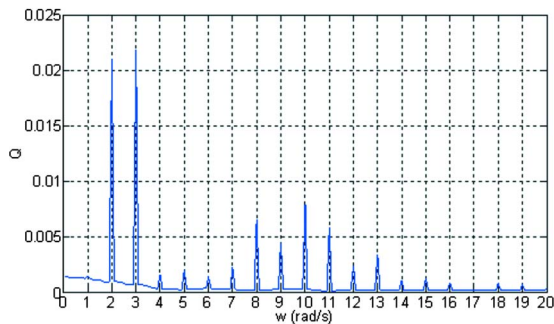


FIG. 9. (Color online) Output response (or spike train) of FHN neuron with $A=0.02$, $\omega_1=2$ rad/s, $\omega_2=3$ rad/s, and $\varepsilon=0.01$.



(a)



(b)

FIG. 10. (Color online) Output spectra with $\varepsilon=0.01$. (a) Theoretical output spectra calculated by Eq. (14). (b) Fourier output spectra derived by simulations.

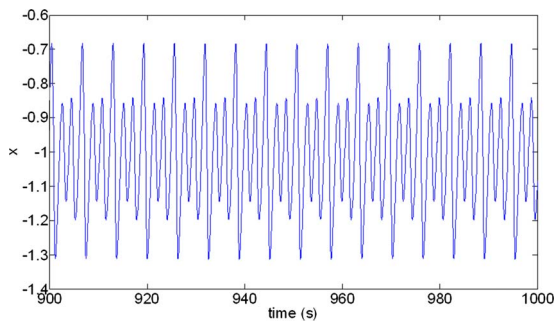
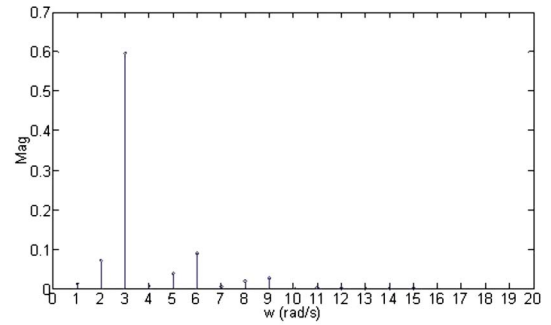
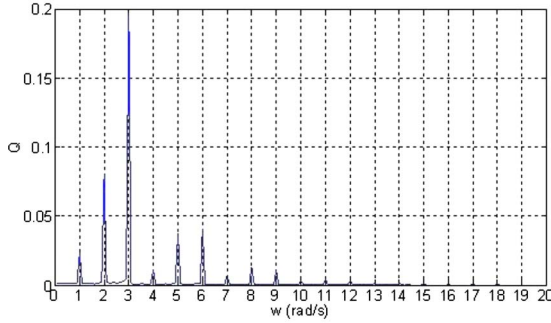


FIG. 11. (Color online) Output response (or spike train) of FHN neuron with $A=0.02$, $\omega_1=2$ rad/s, $\omega_2=3$ rad/s, and $\varepsilon=0.1$.



(a)



(b)

FIG. 12. (Color online) Output spectra with $\varepsilon=0.1$. (a) Theoretical output spectra calculated by Eq. (14). (b) Fourier output spectra derived by simulations.

$$H_4(\omega_1, \omega_2, \omega_3, \omega_4) = -(\alpha_4 + \beta_4)/(24\varepsilon(j(\omega_1 + \omega_2 + \omega_3 + \omega_4))^2 + 24j(a^2 - 1)(\omega_1 + \omega_2 + \omega_3 + \omega_4) + 24).$$

3. Fifth order frequency response function

$$\begin{aligned} \alpha_5 = & -2a(48\pi j(f_1 + f_2 + f_3 + f_4 + f_5) \\ & \times (H_1(f_1)H_4(f_2, f_3, f_4, f_5) + H_1(f_2)H_4(f_1, f_3, f_4, f_5) \\ & + H_1(f_3)H_4(f_1, f_2, f_4, f_5) + H_1(f_4)H_4(f_1, f_2, f_3, f_5) \\ & + H_1(f_5)H_4(f_1, f_2, f_3, f_4)) - 48\pi a j(f_1 + f_2 + f_3 + f_4 \\ & + f_5)(H_2(f_1, f_2)H_3(f_3, f_4, f_5) + H_2(f_1, f_3)H_3(f_2, f_4, f_5) \\ & + H_2(f_1, f_4)H_3(f_2, f_3, f_5) + H_2(f_1, f_5)H_3(f_2, f_3, f_4) \\ & + H_2(f_2, f_3)H_3(f_1, f_4, f_5) + H_2(f_2, f_4)H_3(f_1, f_3, f_5) \\ & + H_2(f_2, f_5)H_3(f_1, f_3, f_4) + H_2(f_3, f_4)H_3(f_1, f_2, f_5) \\ & + H_2(f_3, f_5)H_3(f_1, f_2, f_4) + H_2(f_4, f_5)H_3(f_1, f_2, f_3)), \end{aligned}$$

$$\begin{aligned} \beta_5 = & 24\pi j(f_3 + f_4 + f_5)H_1(f_1)H_1(f_2)H_3(f_3, f_4, f_5) \\ & + 24\pi j(f_2 + f_4 + f_5)H_1(f_1)H_1(f_3)H_3(f_2, f_4, f_5) \\ & + 24\pi j(f_2 + f_3 + f_5)H_1(f_1)H_1(f_4)H_3(f_2, f_3, f_5) \\ & + 24\pi j(f_2 + f_3 + f_4)H_1(f_1)H_1(f_5)H_3(f_2, f_3, f_4) \\ & + 24\pi j(f_1 + f_4 + f_5)H_1(f_2)H_1(f_3)H_3(f_1, f_4, f_5) \\ & + 24\pi j(f_1 + f_3 + f_5)H_1(f_2)H_1(f_4)H_3(f_1, f_3, f_5) \\ & + 24\pi j(f_1 + f_3 + f_4)H_1(f_2)H_1(f_5)H_3(f_1, f_3, f_4) \\ & + 24\pi j(f_1 + f_2 + f_5)H_1(f_3)H_1(f_4)H_3(f_1, f_2, f_5) \end{aligned}$$

$$\begin{aligned}
& + 24\pi j(f_1 + f_2 + f_4)H_1(f_3)H_1(f_5)H_3(f_1, f_2, f_4) \\
& + 24\pi j(f_1 + f_2 + f_3)H_1(f_4)H_1(f_5)H_3(f_1, f_2, f_3) \\
& + 16\pi j f_5 H_1(f_5)H_2(f_1, f_2)H_2(f_3, f_4) \\
& + 16\pi j f_4 H_1(f_4)H_2(f_1, f_2)H_2(f_3, f_5) \\
& + 16\pi j f_3 H_1(f_3)H_2(f_1, f_2)H_2(f_4, f_5) \\
& + 16\pi j f_5 H_1(f_5)H_2(f_1, f_3)H_2(f_2, f_4) \\
& + 16\pi j f_4 H_1(f_4)H_2(f_1, f_3)H_2(f_2, f_5) \\
& + 16\pi j f_2 H_1(f_2)H_2(f_1, f_3)H_2(f_4, f_5) \\
& + 16\pi j f_5 H_1(f_5)H_2(f_1, f_4)H_2(f_2, f_3) \\
& + 16\pi j f_3 H_1(f_3)H_2(f_1, f_4)H_2(f_2, f_5) \\
& + 16\pi j f_2 H_1(f_2)H_2(f_1, f_4)H_2(f_3, f_5) \\
& + 16\pi j f_4 H_1(f_4)H_2(f_1, f_5)H_2(f_2, f_3) \\
& + 16\pi j f_1 H_1(f_1)H_2(f_2, f_4)H_2(f_3, f_5) \\
& + 16\pi j f_1 H_1(f_1)H_2(f_2, f_5)H_2(f_3, f_4) \\
& + 16\pi j f_3 H_1(f_3)H_2(f_1, f_5)H_2(f_2, f_4) \\
& + 16\pi j f_2 H_1(f_2)H_2(f_1, f_5)H_2(f_3, f_4) \\
& + 16\pi j f_1 H_1(f_1)H_2(f_2, f_3)H_2(f_4, f_5),
\end{aligned}$$

$$\begin{aligned}
H_5(f_1, f_2, f_3, f_4, f_5) = & -(\alpha_5 + \beta_5)/(120\varepsilon(2\pi j(f_1 + f_2 + f_3 \\
& + f_4 + f_5))^2 + 240\pi j(a^2 - 1)(f_1 + f_2 \\
& + f_3 + f_4 + f_5) + 120).
\end{aligned}$$

- ¹S. A. Billings and K. M. Tsang, *Mech. Syst. Signal Process.* **3**, 319 (1989).
- ²S. A. Billings and K. M. Tsang, *Mech. Syst. Signal Process.* **3**, 341 (1989).
- ³E. Bedrosian and S. O. Rice, *Proc. IEEE* **59**, 1688 (1971).
- ⁴K. Seluakumaran, W. H. A. M. Mulders, and D. Robertson, *Hear. Res.* **243**, 35 (2008).
- ⁵S. P. Bhagat and C. A. Champlin, *Hear. Res.* **193**, 51 (2004).
- ⁶V. Zemon and F. Ratliff, *Biol. Cybern.* **50**, 401 (1984).
- ⁷S. J. Aiken and T. W. Picton, *Hear. Res.* **245**, 35 (2008).
- ⁸Th. Meigen, R. Prüfer, S. Reime, and A. Friedrich, *Vision Res.* **45**, 2862 (2005).
- ⁹A. N. Lukashkin and I. J. Russell, *Hear. Res.* **203**, 45 (2005).
- ¹⁰M. C. Liberman, J. Zuo, and J. J. Guinan, Jr., *J. Acoust. Soc. Am.* **116**, 1649 (2004).
- ¹¹M. A. Cheatham, K. H. Huynh, J. Gao, J. Zuo, and P. Dallos, *J. Physiol. (London)* **560**, 821 (2004).
- ¹²J. Wang, W. Si, and H. Li, *Chaos, Solitons Fractals* **39**, 28 (2009).
- ¹³S. Bahar and F. Moss, *Chaos* **13**, 138 (2003).
- ¹⁴H. Kitajima and J. Kurths, *Chaos* **15**, 023704 (2005).
- ¹⁵Y. Wu, Y. Shang, M. Chen, C. Zhou, and J. Kurths, *Chaos* **18**, 037111 (2008).
- ¹⁶M. Jiang and P. Ma, *Chaos* **19**, 013115 (2009).
- ¹⁷Y. Xiao, W. Xu, X. Li, and S. Tang, *Chaos* **19**, 013131 (2009).
- ¹⁸T. Pereira, M. S. Baptista, and J. Kurths, *Phys. Rev. E* **75**, 026216 (2007).
- ¹⁹D. Bin, W. Jiang, and F. Xiangyang, *Chaos, Solitons Fractals* **29**, 182 (2006).
- ²⁰M. Schetzen, *The Volterra and Wiener Theories of Nonlinear Systems* (Wiley, New York, 1980).
- ²¹L. O. Chua and C. Y. Ng, *IEEE Electronic Circuits and Systems* **3**, 165 (1979).
- ²²J. J. Bussgang, L. Ehrman, and J. W. Graham, *Proc. IEEE* **62**, 1088 (1974).
- ²³E. I. Volkov, E. Ullner, A. A. Zaikin, and J. Kurths, *Phys. Rev. E* **68**, 026214 (2003).
- ²⁴L. Gammaitoni, P. Hänggi, P. Jung, and F. Marchesoni, *Rev. Mod. Phys.* **70**, 223 (1998).
- ²⁵L. Ning and W. Xu, *Physica A* **382**, 415 (2007).